Journal of Applied Polymer Science

Peroxide induced cross-linking by reactive melt processing of two biopolyesters: Poly(3-hydroxybutyrate) and poly(L-lactic acid) to improve their melting processability

Liqing Wei, Armando G. McDonald
Renewable Materials Program, Department of Forest, Rangeland and Fire Sciences, University of Idaho, Moscow, Idaho 83844-1132
Correspondence to: A. G. McDonald (E-mail: armandm@uidaho.edu)

ABSTRACT: Poly(3-hydroxybutyrate) (PHB) and poly(L-lactic acid) (PLLA) were individually cross-linked with dicumyl peroxide (DCP) (0.25–1 wt %) by reactive melt processing. The cross-linked structures of the polymer gel were investigated by nuclear magnetic resonance (NMR) and Fourier transform infrared (FTIR) spectroscopies. The size of the polymer crystal spherulites, glass transition temperature (T_g), melting transition temperature (T_m), and crystallinity were all decreased as a result of cross-linking. Cross-linking density (v_e) was shown to increase with DCP concentration. Based on parallel plate rheological study (dynamic and steady shear), elastic and viscous modulus (G'' and G'), complex viscosity (η^*) and steady shear viscosity (η) were all shown to increase with cross-linking. Cross-linked PHB and PLLA showed broader molar mass distribution and formation of long chain branching (LCB) as estimated by RheoMWD. Improvements in melt strength offer bioplastic processors improved material properties and processing options, such as foaming and thermoforming, for new applications. © 2014 Wiley Periodicals, Inc. J. Appl. Polym. Sci. **2015**, *132*, 41724.

KEYWORDS: biopolymers and renewable polymers; cross-linking; rheology; thermal properties

Received 23 September 2014; accepted 3 November 2014
DOI: 10.1002/app.41724

INTRODUCTION

Recently, biodegradable and renewably derived polymers have attracted much attention due to the environmental awareness and sustainability issues associated with petroleum-based polymers.[1] Aliphatic polyesters such as poly(D,L-lactic acid) (PLA) and bacterial poly(3-hydroxyalkanoates) (PHAs) including poly(3-hydroxybutyrate) (PHB) and its copolymer [poly(3-hydroxybutyrate-co-3-hydroxyvalerate (PHBV)] are gaining interest due to their renewability, biocompatibility and biodegradability.[2,3] Rather, PLA and PHB are linear polymers, lacking in branches which contributes to their poor melt elasticity as evidenced by low die swell and "neck in," low thermodegradation temperature, and high crystallinity.[4,5] These features, especially the low melt elasticity, limit their processability in cast film extrusion, foaming, blown-film manufacture, thermoforming, and fiber spinning etc. [1,4] Long chain branching (LCB) and polymer chain entanglement in PHB and PLAs can improve their processability.[6] Various methods have been used to introduce cross-links into linear polymer such as copolymerization/blend with other biodegradable polymer blocks,[7,8] radiation induced cross-linking, and peroxide induced cross-linking.[6,9–13] Some of these methods have improved the polymer foaming ability and blown-film processability,[14,15] and the resultant products modified by some of these methods are still biodegradable.[15,16]

Practical cross-linking involves the use of peroxides, which, when used at very low levels, can result in significant increases in melt elasticity. Furthermore, cross-linking, can alter their physical properties such as the crystallinity and transition temperatures.[1] Studies on dicumyl peroxide (DCP) induced cross-linking in carbon black polyethylene and poly(ε-caprolactone) were dependent on reaction temperature, peroxide concentration, and extrusion residence time.[12] Recently the effect of type and amount of peroxide with high-, moderate-, and low-decomposition rate on cross-linking of PLLA during extrusion was investigated.[17] For the slowly decomposed peroxide, e.g. DCP, the lifetime is relatively close to the residence time of extrusion. DCP has relatively high H abstraction ability, which makes it ideal as a cross-linking agent for plastics. When DCP is exposed to high temperature, it will decompose into cumyloxy radicals, of which 60% formed methyl radicals and acetophenone by β-scission.[17] These free radicals are capable of abstracting H atoms from any tertiary —CH along the PLLA or PHB backbone. The corresponding H abstraction mechanism of PHB and PLLA resulting in cross-linking and chain extension are simplified in Scheme 1. This cross-linking may be expected

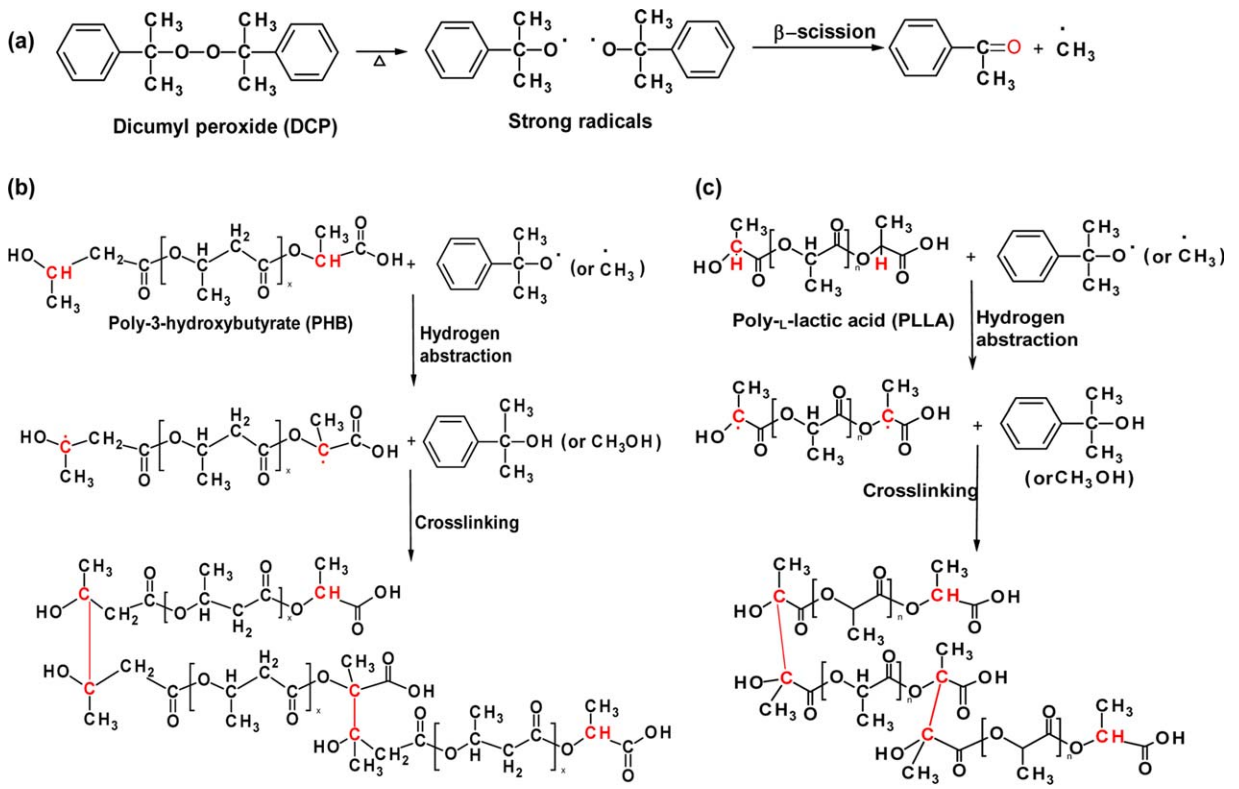

Scheme 1. Schematic illustration of DCP induced cross-linking: (a) thermal decomposition of DCP into primary radicals when exposed to heat and then hydrogen abstraction from polymer chains by primary radicals and bimolecular recombination of polymer radicals of PHB (b) and PLLA (c). [Color figure can be viewed in the online issue, which is available at wileyonlinelibrary.com.]

to occur primarily in the amorphous regions. Melt and rheological properties of the rapidly decomposed lauroyl peroxide and dibenzoyl peroxide cross-linked PLLA were studied.[11] The reductions in crystallinity and improved melt strength of cross-linked PLLA were suitable to be used in conventional melt processing operations including film and foam formation. A PHBV cross-linking study indicated that extensive branching occurred at a DCP concentration above 0.2 wt %.[6] The thermophysical properties such as crystallinity, melting behavior and tensile properties of high-density polyethylene (HDPE) were shown to be influenced by di-tert butyl cumyl peroxide (BCUP) induced cross-linking.[18] The generally accepted process of peroxide induced cross-linking of polymers follows three key steps: (i) the primary radical formation from the thermal decomposition of peroxide, (ii) H abstraction from polymer backbone by free radicals of peroxide generated in step (i), and (iii) the bimolecular radical recombination of polymer radicals from step (ii) to generate C-C cross-links (Scheme 1).[9] Whereas, there is limited information on the chemical position(s) associated with cross-linked molecular chains to form a gel network structure. Moreover, the documentation on the melt rheological properties of PLA and PHAs, especially for peroxide cross-linked PHAs, is limited and therefore instigated this study.

The aims of this study were to cross-link two commercial biopolyesters (PHB and PLLA) by reactive melt processing with DCP, to improve their melt properties and to understand the cross-linking reaction. The cross-linking site of the PLLA and PHB was investigated by ^{13}C NMR spectroscopy. The thermal, viscoelastic, rheological, and morphological properties were evaluated by Fourier transform infrared (FTIR) spectroscopy, DSC, DMA, HS-POM, dynamic rheometry and TGA. To the authors' knowledge, a limited number of reports have used RheoMWD to estimate the molar mass distribution of polymers. This study would provide a profound insight into the structure–property (especially the rheological properties) relationship, induced by cross-linking to improve the industrial processability of PHB and PLLA, broadening the potential applications for these biopolymers.

EXPERIMENTAL

Materials

DCP (98%) was purchased from Sigma-Aldrich Co. LLC (USA). PHB powder was from Tianan Biopolymer (China) and poly(L-lactic acid) (PLLA) was supplied by Purac Biochem (The Netherlands). The weight average molar mass (M_w) and polydispersity (PD) of PHB and PLLA were determined by size exclusion chromatography (SEC) (PHB: $M_w = 290{,}000$ g mol^{-1}, $PD_{SEC} = 2.3$; PLLA: $M_w = 121{,}000$ g mol^{-1}, $PD_{SEC} = 1.41$). SEC separation was performed using a mixed bed Jordi DVB column on elution with $CHCl_3$ (1 mL min^{-1}) with triple detection system [refractive index (Waters model 2414), low-and right-angle laser light scattering and differential viscometer (Viscotek model 270, Viscotek Corporation)].

Cross-Linking via Reactive Melt Processing

PHB and PLLA were dried under vacuum for at least one week before use. Dried PHB powder or PLLA granules (2 g) were placed in a Dynisco laboratory mixing extruder/molder

operating at 175°C for PHB and 190°C for PLLA and melt was mixed (100 revolutions min^{-1}) for 5 min, to which DCP (0, 0.25, 0.5, 1 wt %) was added and mixed for a defined reaction time. All samples were then either injected into a mold (discs or rectangular bars: PHB samples were coded PHB_0, $PHB_{0.25}$, $PHB_{0.5}$ and PHB_1; PLLA samples were coded $PLLA_0$, $PLLA_{0.25}$, $PLLA_{0.5}$ and $PLLA_1$) or extruded into a strand (1 mm Ø).

Gel Fraction and Degree of Swelling in Solvent

Cross-linked polymer networks were not readily soluble in an organic solvent but swelled into a gel. The gel fraction was determined on extruded strands that were refluxed in $CHCl_3$ for 48 h to remove the soluble "sol" fraction by filtration (nylon mesh, 27 μm). The un-dissolved gels induced by 0.25, 0.5, and 1.0 wt % DCP of PHB and PLLA were respectively coded as $PHB_{0.25gel}$, $PHB_{0.5gel}$ and PHB_{1gel}, and $PLLA_{0.25gel}$, $PLLA_{0.5gel}$ and $PLLA_{1gel}$. The cross-linked gel fractions were collected and vacuum dried for 48 h and yields were calculated gravimetrically as follows:

$$\text{Gel fraction } (\%) = \left(W_{gel}/W_0\right) \times 100 \quad (1)$$

where W_0 is the dry weight of the cross-linked polymer, W_{gel} is the weight of dry gel fraction.

Swelling experiments of dry gels (50 mg) were performed in $CHCl_3$ (50 mL) at room temperature (21°C) for 48 h. The degree of swelling (DS, $cm^3\ cm^{-3}$) was calculated by:

$$DS = \left[\left(W_s - W_{gel}\right)/W_{gel}\right] \times \left(\rho_{ap}/\rho_{chloroform}\right) \quad (2)$$

where W_{gel} is the weight of dry gel in the cross-linked polymer sample, W_s is the weight of swollen gel sample (W_s), while ρ_{ap} and $\rho_{chloroform}$ are densities of amorphous polymers (1.248 g cm^{-3} for PLA; 1.179 g cm^{-3} for PHB)[12,19] and $CHCl_3$ (1.48 g cm^{-3}), respectively.

NMR Spectroscopy

Cross-linked $PHB_{0.25gel}$ and $PLLA_{0.25gel}$ gels were partially depolymerized by methanolysis (3% H_2SO_4 in CH_3OH (3 mL) + $CHCl_3$ (1 mL) at 100°C for 8 h) without cleaving the C—C cross-links. The resulting methyl esters were soluble in $CDCl_3$ for nuclear magnetic resonance (NMR) analysis. Standard ^{13}C and DEPT-135 (distortionless-enhancement-by-polarization-transfer) NMR spectra were obtained on a Bruker Avance 500 spectrometer.

FTIR Spectroscopy

Vacuum dried PHB_0, $PLLA_0$, $PHB_{0.25\text{-}1gel}$ and $PLLA_{0.25\text{-}1gel}$ samples were characterized by FTIR spectroscopy (Avatar 370 FTIR spectrometer, ThermoNicolet) using a ZnSe attenuated total reflection (ATR) probe. Absorbance spectra (in triplicate) were averaged and ATR and baseline corrected using Omnic v9.0 software (Thermo scientific).

For the quantitative analysis, the spectra were normalized and curve-fitted using Igor Prof 6.03 software (WaveMetrics).[20] The area (A) of each band found by curve fitting was integrated by the software. The carbonyl index ($I_{C=O}$) was calculated as the ratio of the areas (A) under carbonyl (C=O) bands at 1720–1740 cm^{-1} of PHB ($I_{C=O} = A_{1720}/A_{1740}$), while the CH stretching index (I_{C-H}) was determined by the ratio of areas of —CH (~2882 cm^{-1}) to —CH_3 (asym, ~2946 cm^{-1}) bands of PLLA ($I_{C-H} = A_{2882}/A_{2946}$).

Differential Scanning Calorimetry

Temperature modulated DSC (TMDSC) measurements were conducted on PHB_0, $PLLA_0$, $PHB_{0.25\text{-}1gel}$, and $PLLA_{0.25\text{-}1gel}$ samples using a TA Instruments model Q200 DSC with refrigerated cooling. All samples were first rapidly heated to 200°C (100°C min^{-1}) to remove thermal history followed by a cooling scan (−20°C min^{-1}) to −50°C. Then TMDSC measurements were obtained for heating scans from −50 to 200°C, at an average heating rate of 2°C min^{-1} with a period of 60 s and modulation amplitudes of ±0.6°C. The data were analyzed using TA Universal Analysis v4.4A software. The cold crystallization temperature (T_c) was determined from the cooling scan curve. From the heat capacity data curve, T_g, T_m, and enthalpy of fusion (ΔH_m) were determined. The degree of crystallinity (χ_c %) of PHB and PLLA were calculated based on eq. (3):[21]

$$\chi_c\% = \left(\Delta H_m - \Delta H_{crys+recrys}\right)/\Delta H_0 \times 100 \quad (3)$$

where ΔH_m is the melting enthalpy (reversing curve), the $\Delta H_{crys+recrys}$ is the sum of exotherms of crystallization (reversing) and recrystallization (non-reversing), and ΔH_0 is melting enthalpy in J g^{-1} of 100% crystalline PHB (146 J g^{-1}) and PLLA (93.6 J g^{-1}).[3,22] The heat flow data from the TMDSC scans were used to calculate the variation of specific heat capacity (ΔC_p, J $g^{-1}{}^{\circ}C^{-1}$) close to the glass state at which T_g was determined.

Hot Stage-Polarized Optical Microscopy (HS-POM)

PHB_0 and $PLLA_0$ films (cast from $CHCl_3$ solution ~ 1 mg mL^{-1}) and the cross-linked $PHB_{0.25\text{-}1gel}$ and $PLLA_{0.25\text{-}1gel}$ films were prepared by hot pressing at 180°C. Films were used for morphological studies on isothermally formed crystals using an Olympus BX51 microscope [10× objective, polarized light filters and digital camera (Olympus DP70)] equipped with a Mettler Toledo FP900 Thermosystem (FP90 central processor and FP84 hot stage). Samples were first heated at 20°C min^{-1} to 190°C, held for 2 min, then cooled at −20°C min^{-1} to the desired temperature (90°C), and held isothermally for 1 h.[23] All images were processed using the Olympus MicroSuite (TM)-SE 3.2 software.

Thermogravimetric Analysis (TGA)

Thermal stability of PHB_0, $PLLA_0$, $PHB_{0.25\text{-}1gel}$, and $PLLA_{0.25\text{-}1gel}$ samples (3–5 mg) were characterized using a Perkin Elmer TGA 7 instrument (50–900°C at 20°C min^{-1} under N_2 flow) and data were analyzed using Pyris v8 software.

Dynamic Mechanical Analysis (DMA)

The flexural properties of molded bars (60 mm × 4 mm × 2 mm) for PHB_{0-1} and $PLLA_{0-1}$ samples were dried under vacuum for 24 h and then conditioned (25°C, 50% relative humidity) for 7 days. DMA was carried out using a DMA model Q800 instrument (TA instrument) to determine the viscoelastic properties in 3-point bending mode (50-mm span) from −50 to 150°C at 3°C min^{-1}, 0.5% strain, and at 1 Hz.

Parallel Plate Rheometry

Steady shear (η) and dynamic measurements (G', G'', and η^*) were determined using a Bohlin Instuments CVO 100 rheometer, parallel plate (25 mm Ø), in oscillating shear mode with an

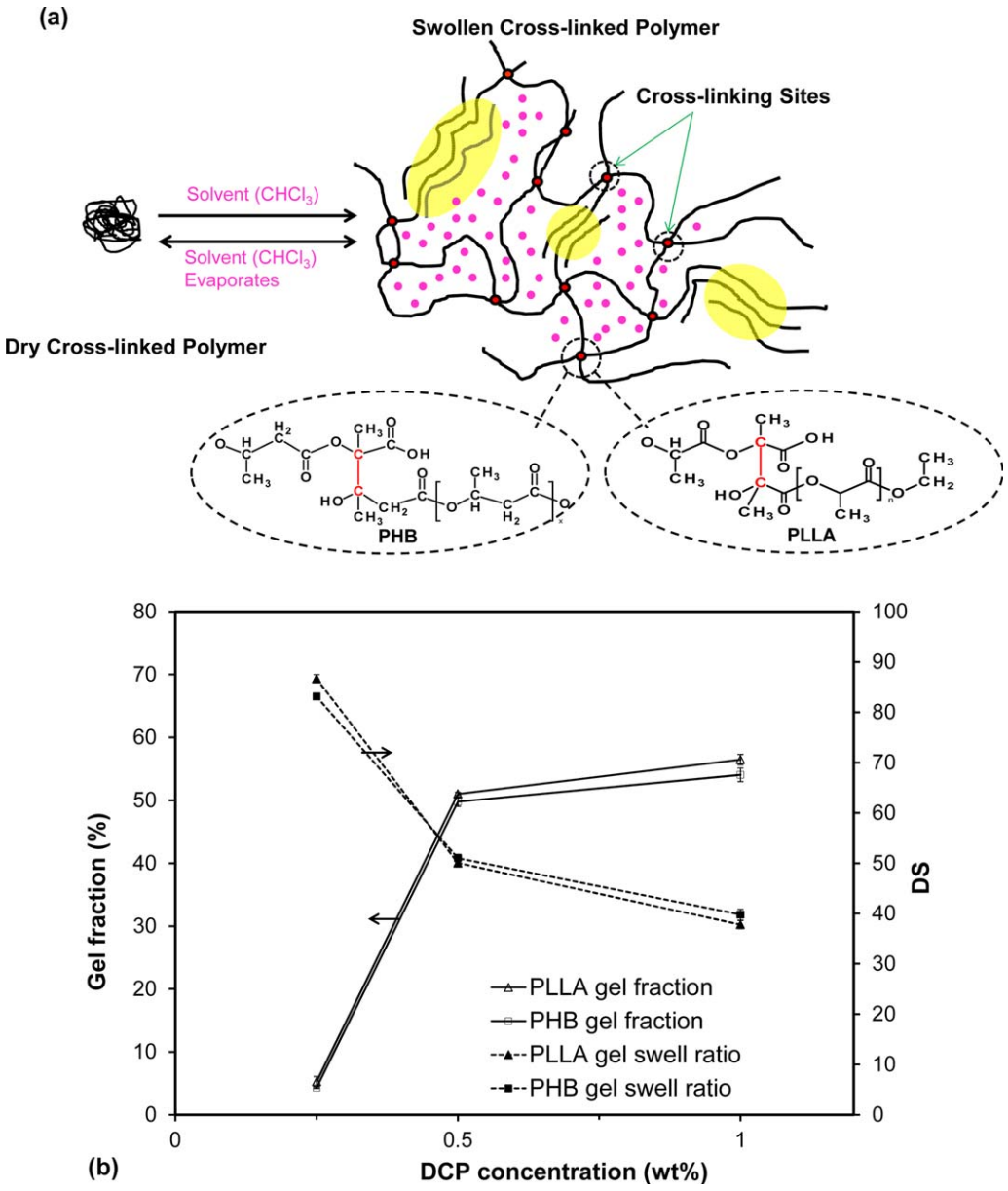

Figure 1. (a) A model of cross-linked polymer gels swelling in solvent (note: polymer chains (black) comprising crystalline (yellow shadow) and amorphous domains cross-linked at sites (red) allow the cross-linked network to expand in contact with the solvent (e.g., $CHCl_3$) and will be incorporated with solvent molecules (pink); (b) Gel fraction (%) and DS of cross-linked $PHB_{0.25\text{-}1}$ (8 min) and $PLLA_{0.25\text{-}1}$ (10 min) extruded strands as function of DCP concentration (0.25, 0.5, and 1 wt %). (Note: the results were averaged from 3 replicates with standard error showed as error bars). [Color figure can be viewed in the online issue, which is available at wileyonlinelibrary.com.]

ETC module on molded discs (2 mm × 25 mm Ø) samples ($PHB_{0–1}$ and $PLLA_{0–1}$). Experiments were performed in the linear viscoelastic region. For PHB measurements these were carried out at 170, 175, and 180°C, while for PLLA these were performed at 180, 190, and 200°C. Steady shear measurements were undertaken at shear rates (γ) from 0.1 to 100 s^{-1}, while dynamic measurements were conducted in the frequency range of 0.1–100 rad/s at an applied strain of 0.5%. Data were analyzed using the Bohlin rheology v6.51 software.

An estimation of molecular PD was determined by RheoMWD 1.5 software (Polydynamics, Canada) using a viscosity function method from dynamic rheology data (G' and G'' as function of frequency). Four PD measures were recorded: the crossover point index (CPI), global distribution index (GDI), high elasticity index (HEI) and Dow rheology index (DRI). In this analysis, the temperature dependence factor (TDF) for same material was required. Step one is to calculate PD measures for all materials using the same value of the TDF at three different temperatures (listed above). If the calculated PD measures were almost the same as the correct TDF value then TDF will be changed and PD measures recalculated until the calculated PD measures are the same. The viscosity function method uses the steady

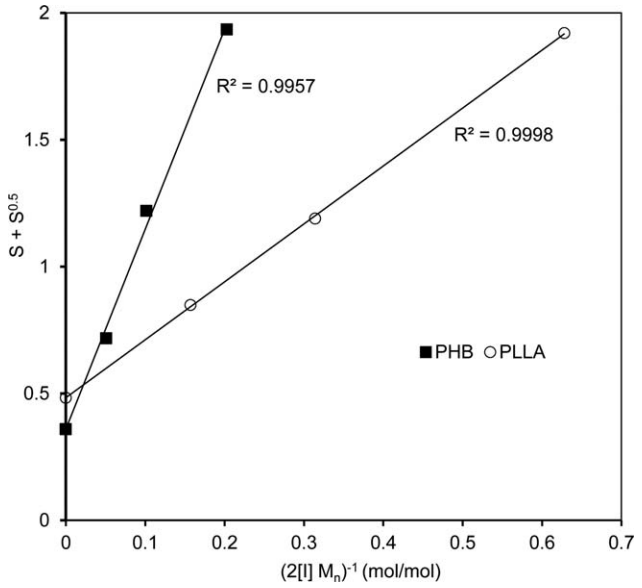

Figure 2. Charlesby-Pinner plot of the cross-linking of PHB at 175°C for 8 min and PLLA at 190°C for 10 min with DCP concentration.

shear viscosity data [viscosity (η) vs. shear rate at a single temperature] to estimate the PD ($=M_w/M_n$) as a molar mass distribution indicator.

RESULTS AND DISCUSSION

PLLA and PHB Cross-Linking via Reactive Melt Processing with Dicumyl Peroxide

Cross-linked PHB and PLLA materials form covalently tied networks, are insoluble gels, and are only swollen in contact with solvents [Figure 1(a)].[24] Factors that influence cross-linking in the gel fraction are reaction time and DCP concentration. Experiments showed that the gel fraction increased with reaction time up to 8 min for PHB and 10 min for PLLA. However, when reaction time was extended, the gel fraction decreased. The gel fraction for PHB increased from 4 to 58%, while for PLLA increased from 5 to 59% when DCP concentration increased from 0.25 to 1 wt % [Figure 1(b)]. The DS is a good indicator of cross-linking density of polymers. The DS of both PHB and PLLA decreased with DCP concentration [Figure 1(b)]. These results support that cross-linking occurred and the extent of cross-linking was DCP concentration dependent.

At 175°C for PHB and 190°C for PLLA chain scission will accompany cross-linking reactions and at long reactions times the gel fraction will decrease. The efficiency of cross-linking can be determined from the Charlesby-Pinner equation [eq. (4)], when there are both cross-linking and chain scissioning present, as follows:[17]

$$S+S^{0.5}=p_0/q_0+\ (2M_n[I])^{-1}(E_c)^{-1} \qquad (4)$$

where S is the soluble fraction, p_0 and q_0 are the fractions of the repeat units of polymer undergoing scissioning and cross-linking, respectively, M_n is the number-average molar mass of the polymer before cross-linking, $[I]$ is the decomposed peroxide in mol/g polymer, $(2M_n[I])^{-1}$ is the mole ratio of radicals to polymer chains in our work, and E_c is the cross-linking efficiency. The Charlesby-Pinner plot of $S+S^{0.5}$ against $(2M_n[I])^{-1}$ for different levels of DCP are shown in Figure 2. The intercept of $S+S^{0.5}$ axis gives the ratio of the chain scissioning and cross-linking, p_0/q_0, which are 0.48 for PHB and 0.36 for PLLA, indicating chain scissioning occurs under their corresponding processing temperatures. It was possible that some chain scissioning was attributed to thermal instability of the linear polymer.[25] The E_c is given by 1/slope which was calculated at 7.88 for PHB and 2.28 for PLLA. These data suggest that a higher DCP concentration is required for PLLA than PHB if a comparable cross-linking density is to be obtained.

Characterization by NMR

The cross-linking sites for PHB and PLLA were investigated by ^{13}C NMR experiments on the methanolyzed $PHB_{0.25gel}$ and $PLLA_{0.25gel}$. As proposed (Scheme 1), for both PHB and PLLA cross-linking would occur at the tertiary C to form a quaternary C. A standard ^{13}C NMR spectrum of cross-linked PHB showed two quaternary C signals at δ 172.2 ppm (C═O) and 70.5 ppm which disappeared in DEPT-135 spectrum [Figure 3(a)], supports the PHB cross-linking site outlined in Scheme 1. The methanolyzed $PLLA_{0.25gel}$ showed quaternary C signals at δ 176.0 ppm (C═O) and 97.0 ppm in the ^{13}C spectrum and disappeared in the DEPT-135 [Figure 3(b)] which supports the PLLA cross-linking site (Scheme 1). Therefore it is concluded that the cross-linking did occur for PHB and PLLA polymers with DCP.

Quantitative Analysis by FTIR

The crystallinity of PHB and PLLA will decrease due to cross-linking and this was monitored by FTIR spectroscopy (Figure 4). The intensities of bands at 980, 1226, 1278 cm^{-1} from the PHB crystalline phase were shown to decrease with cross-linking, the band at 1181 cm^{-1} associated with the amorphous phase was shown to increase [Figure 4(a)].[25] The broad band between 1800 and 1650 cm^{-1} was assigned to carbonyl stretching of the PHB polymer and was processed by peak fitting to obtain better band assignments [Figure 4(a)]. The fitted bands at 1720 and 1740 cm^{-1} were assigned to the stretching vibration of the crystalline and amorphous ester carbonyl groups, respectively [Figure 4(a)].[25] Due to cross-linking the band intensity increased at 1720 cm^{-1} and the shoulder at 1740 cm^{-1} increased relative to 1720 cm^{-1} band. These results show that the amorphous PHB level increased with the extent of cross-linking. To quantify this change related to crystallinity, the FTIR spectra were imported into Igor Pro software, peak fitted and $I_{C=O}$ was calculated with results summarized in Table I. It can be seen that $I_{C=O}$ values decreased from 1.30 (PHB_0) to 0.39 for PHB_{1gel}.

For PLLA strong IR bands at 2997, 2946, and 2882 cm^{-1} were assigned to the —CH stretching region (—$CH_{3(asym)}$, —$CH_{3(sym)}$, and —CH modes).[26] Due to different levels of cross-linking by DCP the intensity of all these samples were higher than $PLLA_0$ [Figure 4(b)]. For quantitative analysis, the region of CH stretching between 3050 and 2800 cm^{-1} was peak-fitted [Figure 4(b)]. The ratio of the areas of —CH and —CH_3 (sym), I_{C-H}, was obtained (Table I). It was determined that I_{C-H} was 2.27 for $PLLA_0$. When the DCP levels increased to 1 wt % the I_{C-H}

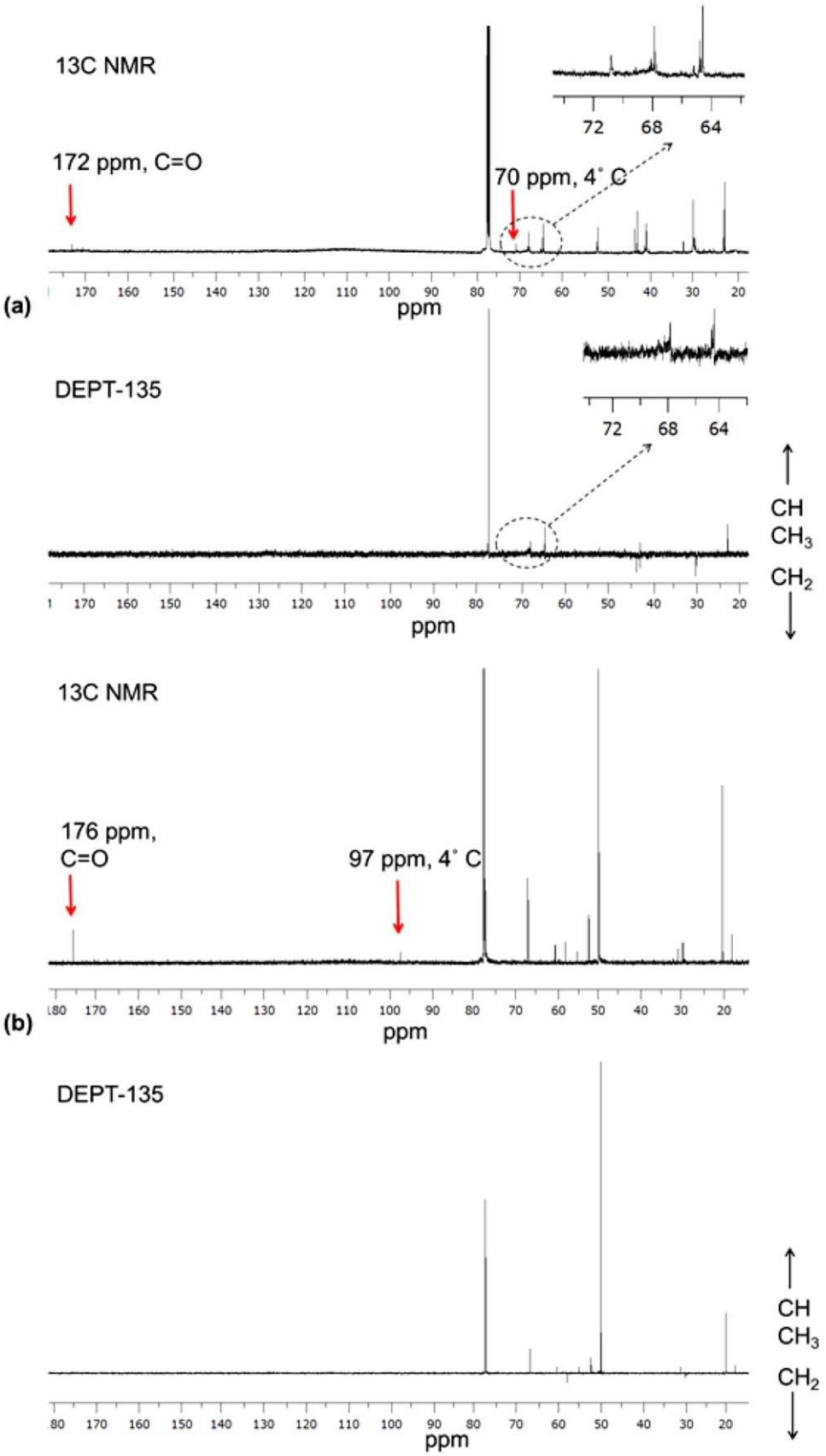

Figure 3. ^{13}C NMR and DEPT-135 spectra of methanolyzed (a) $PHB_{0.25gel}$ and (b) $PLLA_{0.25gel}$. [Color figure can be viewed in the online issue, which is available at wileyonlinelibrary.com.]

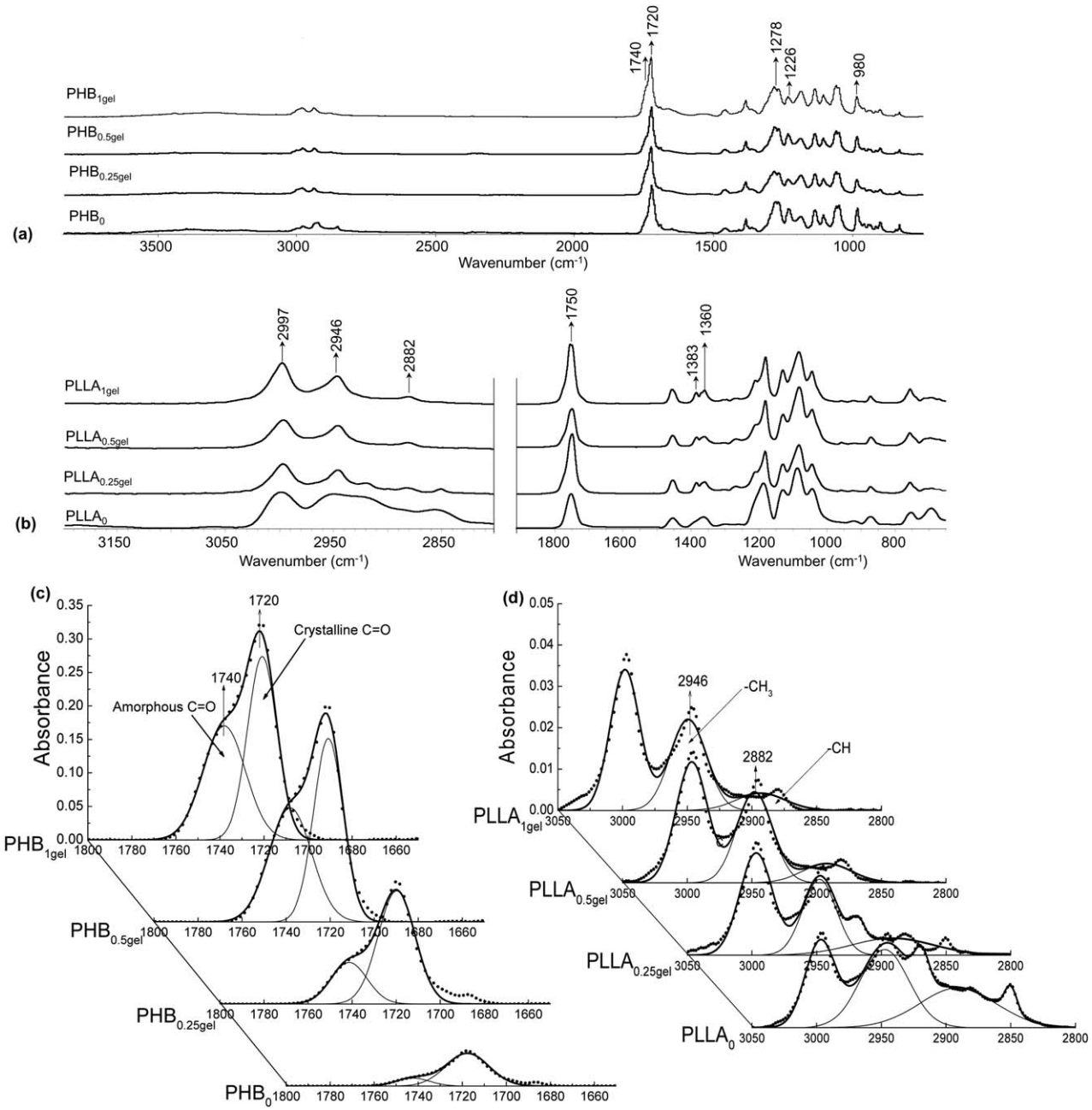

Figure 4. FTIR spectra of (a) PHB_{0-1gel}, (b) $PLLA_{0-1gel}$, (c) curve fitting of carbonyl (C═O) band (1800–1650 cm^{-1}) of PHB_{0-1gel} samples, and (d) curve fitting of ─C─H stretching band (3050–2800 cm^{-1}) of $PLLA_{0-1gel}$ samples.

value was significantly reduced to 0.06. This verified that more PLLA chains were cross-linked together at the methine sites. In other words, less methine groups were present in the cross-linked networks as compared with the methyl groups as outlined in Scheme 1.

DSC Analysis

The polymers were analyzed by TMDSC which allowed for observing the formation of crystalline structures as soon as the polymer starts to melt (recrystallization). The thermal properties of the polymers are listed in Table I. The total heat flow curve (T) of all samples was separated into non-reversing (Non-Rev) and the reversing flow (Rev) curves (Figure 5).[21] The T_g was clearly visible in Rev curves followed by the cold crystallization (exotherm) region after which a melting endotherm peak was observed. From the Non-Rev curves a recrystallization exothermal peak was observed.

The T_g of PHB and PLLA were influenced by DCP concentration (Table I). The PHB_0 and $PLLA_0$ have a T_g at 5.0 and 62.0°C, respectively. The T_g was shown to decrease with the extent of cross-linking. For example, the T_g decreased by 5°C for PHB_{1gel} and 10°C for $PLLA_{1gel}$ as compared with controls. To note, one more transition/relaxation of PHB system (T_{2nd}) was observed at the region below T_g and the onset temperature (T_{2nd}) shifted to lower values [Figure 5(a,b)]. This T_{2nd} was

Table I. The $I_{C=O}$, I_{C-H}, Crystallinity and Thermal Properties of PHB_0, $PLLA_0$, $PHB_{0.25\text{-}1gel}$ and $PLLA_{0.25\text{-}1gel}$ Samples

	PHB_0	$PHB_{0.25gel}$	$PHB_{0.5gel}$	PHB_{1gel}	$PLLA_0$	$PLLA_{0.25gel}$	$PLLA_{0.5gel}$	$PLLA_{1gel}$
$I_{C=O}$	1.30	1.23	0.97	0.39				
I_{C-H}					2.27	0.16	0.07	0.06
T_g (°C)	5.5	4.4	2.2	0.5	62.0	59.0	57.3	52.0
T_{2nd} (°C)	−20.4	−22.0	−24.1	−29.3				
ΔC_p (J g^{-1} °C^{-1})[a]	0.43	0.64	0.70	0.88	0.29	0.37	0.43	0.51
T_c (°C)	93.9	89.0	88.9	86.9	103.0	100.8	95.6	94.9
$\Delta H_{crys+recrys}$ (J g^{-1})[b]	0.36	0.51	4.19	4.29	29.31	13.17	11.08	10.55
T_m (°C)[c]	174.0	170.0	158.1	151.0	176.8	164.0	160.0	159.0
ΔH_m (J g^{-1})[d]	59.48	21.75	8.91	7.94	58.03	18.6	13.48	10.84
χ_c (%)[e]	40.49	14.55	3.23	2.50	31.93	6.43	0.96	0.31

[a] Variation of heat capacity (C_p).
[b] Exothermal enthalpy of crystallization and recrystallization.
[c] Melting temperature determined from the second melting peak (higher temperature) of total heat flow curve (T) as shown in Figure 5.
[d] Melting enthalpy.
[e] Degree of crystallinity determined by eq. (3).

probably attributed to an increased amount of side macromolecular chains of the cross-linked PHB gels. The precise original χ_c of PHB_{1gel} and $PLLA_{1gel}$ reduced significantly to 2.5% and 0.31%, respectively. The decrease of crystallinity (or amorphous phase increase) observed by DSC were supported by FTIR (Table I). Since T_g is directly related to the macromolecular mobility of polymer chains, hence, lower χ_c, the lower the energy required to move the polymer chains in the amorphous phase.[27] Therefore, the temperature to transit the polymer from a glassy to a rubbery state (T_g) will be lowered. For cross-linked PHB and PLLA, the χ_c was low, which explains why T_g and peak of cold crystallinity appeared more clearly than controls (Figure 5). The similar thermal behavior changes were observed for cross-linked PE by BCUP and PHBV by DCP

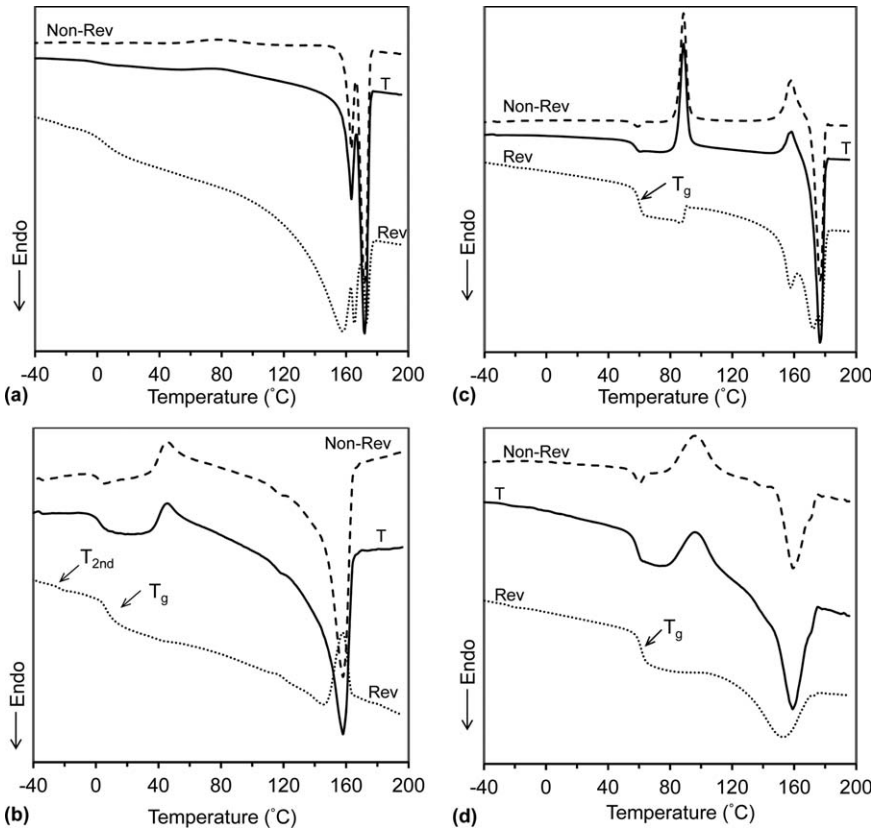

Figure 5. TMDSC thermograms of (a) PHB_0, (b) PHB_{1gel}, (c) $PLLA_0$ and (d) $PLLA_{1gel}$. Three curves for each sample are total heat flow (T), non-reversing (Non-Rev) and reversing (Rev) heat flow.

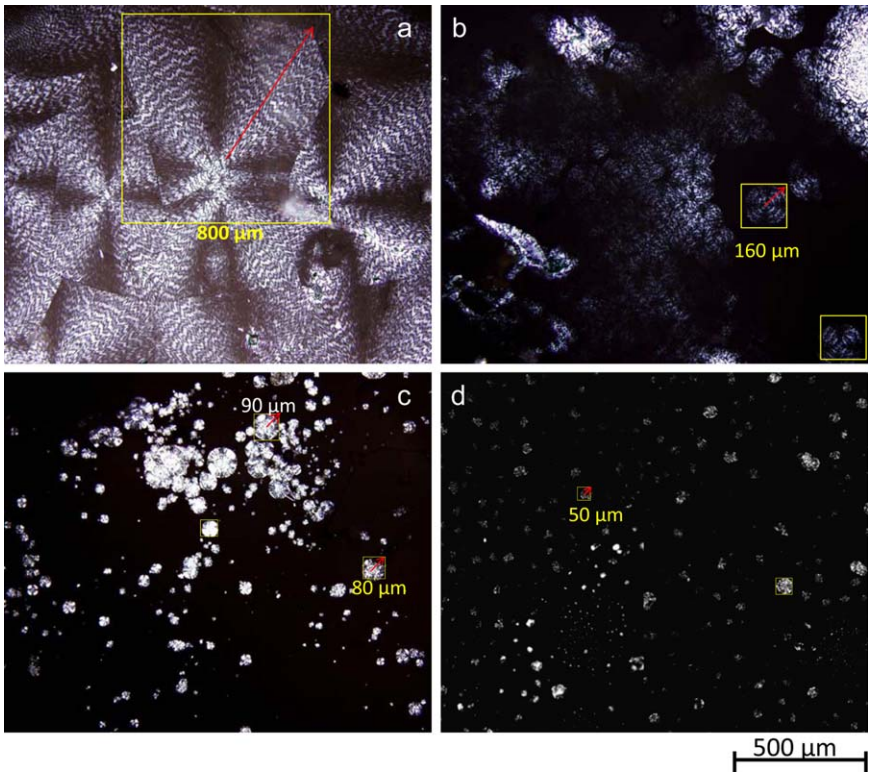

Figure 6. HS-POM micrographs (100×) at 90°C of: (a) solvent cast PHB film, and hot pressed (b) $PHB_{0.25gel}$, (c) $PHB_{0.5gel}$, and (d) PHB_{1gel} films. All the images have the same scale and marked area showed the sizes of spherulites (note: arrow shows the approximate radius). [Color figure can be viewed in the online issue, which is available at wileyonlinelibrary.com.]

respectively.[16,18] Hence, DCP concentration can be adjusted to tune the extent of cross-linking in PHB and PLLA to meet various requirements for T_g and χ_c for different applications.

The heat capacity (ΔC_p) was shown to increase for both PHB (0.43–0.88 J $g^{-1}{}^{\circ}C^{-1}$) and PLLA (0.29–0.51 J $g^{-1}{}^{\circ}C^{-1}$) with increasing DCP concentration or cross-linking density (0.25–1%) (Table I). These changes of ΔC_p due to cross-linking also indicate that more polymer chains entered into amorphous state,[28] which was further verified by the large crystallization peak observed for cross-linked PHB and PLLA (Figure 5). In addition, the T_m and ΔH_m were determined from the endotherm peak of the total and Rev heat flow curves, respectively. For PHB_0 and $PLLA_0$, multiple/double melting peaks were observed, suggesting PHB samples experienced secondary crystallization during TMDSC heating scans under the experimental condition (using cooling rate = 20°C min^{-1}) employed.[29] The peak at higher temperature was considered to be the true melting peak (T_m) representing the original polymer before the DSC experiment. These multiple peaks merged into one single melting peak with an increase of DCP concentration. T_m and ΔH_m (crystalline fraction) for PHB and PLLA were shown to decrease with the extent of cross-linking. The cold crystallization temperature (T_c) of cross-linked PHB and PLLA was also shown to decrease slightly, since the formation of cross-linking networks will disturb the reorganization and chain folding during crystallization process.[18] This phenomenon will result in the formation of small crystallites and thus T_c will decrease accordingly.

Morphology

The crystalline morphologies of PHB and PLLA samples were analyzed by HS-POM after isothermal crystallization from the melt at 90°C (above their T_c as shown in Table I). Figures 6(a) and 7(a) show micrographs of solvent casted PHB and PLLA films showing spherulites with typical birefringent Maltese cross pattern.[23] The control $PLLA_0$ has smaller spherulites (radius about 240 μm) than PHB_0 (radius about 560 μm), while straight boundaries were observed between neighboring spherulites for both of them, indicating the spherulite growth follows the heterogeneous nucleation mechanism.[23] If the isothermal temperature was set about 30°C higher than the T_c then the diameter of PHB_0 spherulite tends to reach to 3000 μm before they impinge each other because the nuclei site are limited. Cross-linking tends to reduce the size of PHB and PLLA spherulites [Figures 6(b–d) and 7(b–d)], because those numerous cross-linking sites performed as nucleation sites. With the increase of cross-linking the polymer chains are constrained against diffusion and conformational rearrangement, hence, higher peroxide loadings give rise to a reduced χ_c and crystal size. Therefore, it could be suggested that cross-linked PHB, and PLLA, will be less brittle than the original polymers due to the decrease in the size of crystals which minimizes crack formation between the spherulites.[30] In other words, the cross-linking would act as a plasticizer or nucleation agent in the final products.

Thermal Stability

Table II reports the starting (onset) decomposition temperature (T_{onset}) and their complete degradation temperature (T_{comp}) for

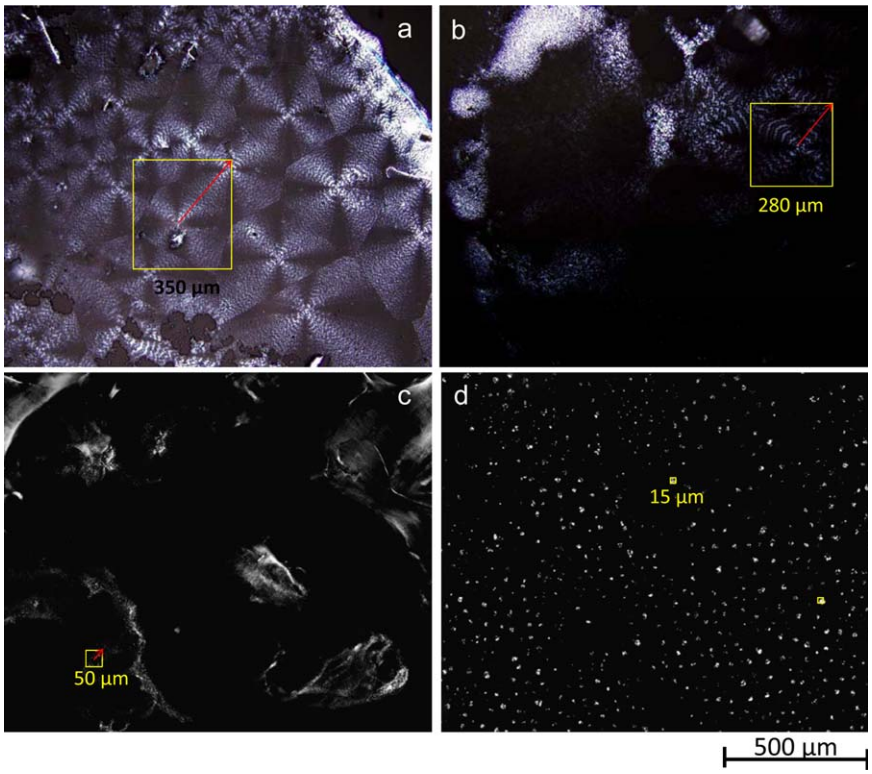

Figure 7. HS-POM micrographs (100×) at 90°C of: (a) solvent cast PLLA film, and hot pressed (b) $PLLA_{0.25gel}$, (c) $PLLA_{0.5gel}$, and (d) $PLLA_{1gel}$ films. All the images have the same scale and marked area showed the sizes of spherulites (note: arrow shows the approximate radius). [Color figure can be viewed in the online issue, which is available at wileyonlinelibrary.com.]

all control and cross-linked PLLA and PHB samples. Degradation (98% mass loss) occurred in one step for all polymers. PHB_0 and $PLLA_0$ started to decompose at 270 and 344°C, respectively. However, cross-linked gels started degradation at higher temperature (>10°C) for both PHB and PLLA. These observations indicate that cross-linked structures improve the thermal stability of PHB and PLLA to some extent, especially for PHB since its thermal instability is one of its drawbacks.[5] Since cross-linking occurred at the tertiary carbons this makes the polymer more prone to thermal decomposition as found for HDPE.[18] Therefore, the observed thermal stability for PHB and PLLA is cross-link dependent and results in fewer tertiary C's for scission.

Viscoelastic Properties

The results of three point bending test of cross-linked PHB and PLLA samples by DMA are shown in Figure 8 and Table III. For both PHB and PLLA only one transition (glass transition or α transition) were seen from the tan δ peak [Figure 8(b,d)], and the transition temperature [tan δ_{max} (°C)] shifted to lower temperatures with the increase of DCP concentration (Table III), indicating the cross-linked PHB became more flexible and the same trend was seen in PLLA. In addition, the maximum values of tan δ (tan δ_{max}) were higher due to cross-linking for both PHB and PLLA (Table III), suggesting higher mobility of cross-linked polymers (reduction in degree of crystallinity) with more side branches were introduced with an increase of DCP concentration and broader polymer structural distribution.[27] The loss modulus (E'') of all cross-linked PHB were shown to have two transitions (α or T_g and β) [Figure 8(a,c)], while the low temperature β transition (around −25°C) was very close to the T_{2nd} of cross-linked gels (around −22 to −29.3°C) as obtained by TMDSC (Table I). The β transition is associated with side chain branching effect in the cross-linked polymer and not observed in PHB_0.[27] No β transition was observed in $PLLA_0$, however, for the cross-linked $PLLA_1$ sample only showed a β transition (between 20 and 35°C). If compared with TMDSC data (Table I), positions of the α transitions detected by DMA seemed to be reasonable (Table III). These results support the findings obtained from the Charlesby-Pinner plot (Figure 2) that higher concentration of DCP is required for cross-linking PLLA than PHB.

Table II. Decomposition Temperatures of PHB_0, $PLLA_0$, $PHB_{0.25\text{-}1gel}$ and $PLLA_{0.25\text{-}1gel}$ Samples Obtained by TGA

Samples	T_{onset} (°C)	T_{comp} (°C)
PHB_0	270	295
$PHB_{0.25gel}$	281	300
$PHB_{0.5gel}$	284	311
PHB_{1gel}	291	313
$PLLA_0$	344	383
$PLLA_{0.25gel}$	356	390
$PLLA_{0.5gel}$	359	391
$PLLA_{1gel}$	361	392

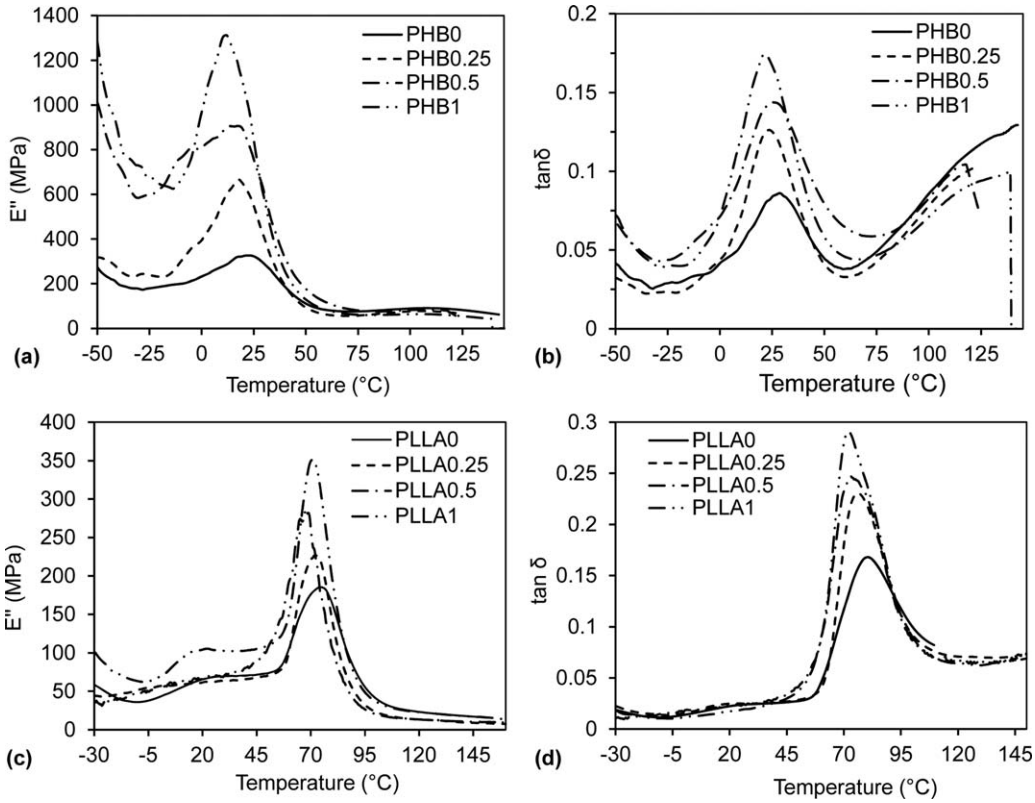

Figure 8. DMA thermograms showing the effect of cross-linking on the (a) loss modulus (E'') and (b) tan δ for PHB_{0-1} samples; (c) loss modulus (E'') and (d) tan δ for $PLLA_{0-1}$ samples.

To confirm these observations, the cross-linking density (v_e) for the obtained networks was calculated (Table III). In this study, the v_e was calculated by the equation derived from the theory of rubber elasticity:[31]

$$E' = 3v_e RT \quad (5)$$

where E' is the storage modulus in the rubbery plateau region from DMA test, R is the gas constant, and T is the absolute temperature. The v_e increased from 1.32 for $PHB_{0.25}$ to 1.88 for PHB_1 (Table III). This illustrated why lower DS was observed with higher DCP concentration. For PLLA samples a similar trend was seen in that the v_e was positively dependent on DCP concentration. The higher E' values were observed for all cross-linked samples within the glassy region of PHB and PLLA as well (Table III), which attributed to the higher v_e and the extra high strength of C—C bonds formed within the cross-linked networks.[32]

Melt Strength and Rheological Properties

Figure 9 shows the dynamic moduli (G' and G'') of PLLA (190°C) and PHB (180°C) and their cross-linked materials under isothermal conditions. For both PLLA and PHB, elasticity (G') and loss modulus (G'') were shown to increase upon cross-linking. For instance, the G' for PHB_0 was shown to increase

Table III. Viscoelastic Properties Obtained by DMA on Three Point Bending Tests for Molded PHB_{0-1} and $PLLA_{0-1}$ Disc Samples

Sample	Tan δ_{max}	Tan δ_{max} (°C)	α transition (°C)[a]	β transition (°C)[a]	E' (MPa)	$v_e \times 10^{-3}$ (mol cm^{-3})
PHB_0	0.08	29	22	None	5644	0.83
$PHB_{0.25}$	0.12	24	20	−26	8968	1.32
$PHB_{0.5}$	0.14	24	10	−28	11459	1.68
PHB_1	0.18	21	6	−29	12838	1.88
$PLLA_0$	0.18	77	75	None	2372	0.29
$PLLA_{0.25}$	0.20	73	73	None	2739	0.34
$PLLA_{0.5}$	0.24	71	68	−30	2942	0.37
$PLLA_1$	0.28	70	70	−29	3613	0.45

[a] α (T_g) and β transitions were determined from E'' as shown in Figure 9(a,c).
None: No transition was observed.

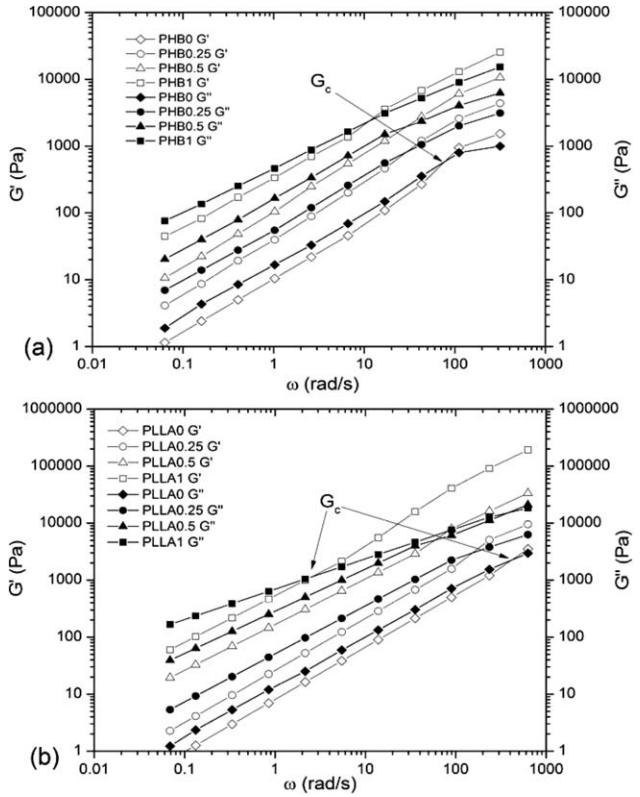

Figure 9. Effect of DCP concentration on dynamic rheology storage (G') and loss (G'') moduli of (a) PHB_{0-1} samples at 180°C and (b) $PLLA_{0-1}$ samples at 190°C.

from 10 to 200 Pa (PHB_1) at 1 rad/s. At lower frequency (ω, rad/s) the G' was lower than G'', indicating that the polymers were liquid-like. The cross-over point of G' and G'' ($G_c = G' = G''$) was shown to occur at a lower frequency for the cross-linked polymers than for PHB_0 and $PLLA_0$. The G_c decreased from 90 rad/s for PHB_0 to 10 rad/s for PHB_1 [Figure 9(a)]. A similar trend was observed between $PLLA_0$ to $PLLA_{0.5}$ while $PLLA_1$ had a much lower G_c value [Figure 9(b)]. Positive correlations between G_c and D (or M_w/M_n and M_z/M_n) has previously been reported for other linear polymers.[33] The G' and G'' values of cross-linked $PHB_{0.25\text{-}1}$ and $PLLA_{0.25\text{-}1}$ were higher than PHB_0 and $PLLA_0$ polymers which clearly show that melt strength was significantly increased by a higher level of LCB and cross-linking density.[6] The low level of elasticity for PHB_0 and $PLLA_0$ compared with cross-linked polymers was caused by their higher chain stiffness and this phenomenon is in accordance with higher T_g and T_m for the linear polymers.

The viscosity (η and η^*) of PLLA and PHB were shown to increase significantly with the extent of cross-linking (Figure 10). For example, η^* for PHB increased from 30 (PHB_0) to 1000 Pa·s for PHB_1 (at 0.1 rad/s) upon cross-linking. For PHB_0 and $PLLA_0$, the viscosity curves (η and η^*) show a Newtonian plateau when γ <10 Hz, while the γ >10 Hz, shear thinning was observed [Figure 10(a)]. The cross-linked $PHB_{0.25\text{-}1}$ polymers have a higher PD and therefore have a broad transition range (shear rate) where shear thinning occurs. This trend was similar to the cross-linked PLLA samples [Figure 10(b)]. Since the shear thinning behavior is associated with a decrease of entanglement and network density and/or polymer chains dissociation by shear during extrusion, PHB experienced more shear thinning than PLLA.[34]

Dynamic rheological data were analyzed using the RheoMWD Polydispersity Measures software to further understand polymer chain entanglement. TDF values for PHB and PLLA were estimated to be 0.99 and 0.9, respectively. The RheoMWD incorporates four measures of PD, which are CPI, HEI, GDI and DRI. Each of these indices was derived from frequency data in the linear viscoelastic region and calculated values are given in Table IV. The HEI values were higher for cross-linked $PHB_{0.25\text{-}1}$ and $PLLA_{0.25\text{-}1}$ samples compared with linear PHB_0 and $PLLA_0$. The HEI term was introduced specifically for characterizing the breadth of molar mass distribution. Note: HEI was designed to quantify high molar mass PD and/or the LCB at the higher molar mass end, and HEI has no contributions at low molar mass.[35] Therefore, these results indicate that cross-linked PHB and PLLA have broader MWD at the high molar mass end than linear PHB and PLLA, respectively. The GDI term was affected by both the high molar mass component (M_z/M_w) as well as the low molar mass component (M_w/M_n). From the HEI values it

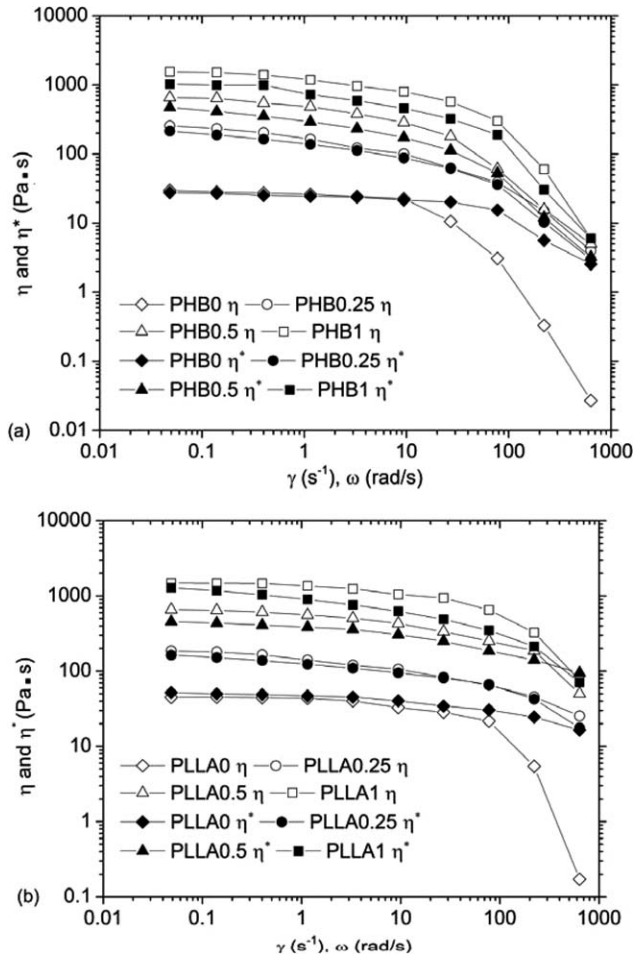

Figure 10. Dynamic rheology showing complex viscosity (η^*) as a function of frequency (ω, rad/s) and steady shear viscosity (η) as a function of shear rate (γ, s^{-1}) of (a) PHB_{0-1} samples at 180°C and (b) $PLLA_{0-1}$ samples at 190°C.

Table IV. Computed PD Measures and MWD for $PHB_{0–1}$ and $PLLA_{0–1}$ Samples by RheoMWD

Sample	M_w/M_n	TDF	CPI	GDI	HEI	DRI
PHB_0	2.01	0.99	7.78	2.15	2.11	120
$PHB_{0.25}$	3.23	0.99	14.1	10.0	2.53	165
$PHB_{0.5}$	3.45	0.99	41.1	30.0	4.34	132
PHB_1	4.56	0.99	50.5	40.1	6.21	353
$PLLA_0$	1.46	0.90	6.72	2.42	1.18	109
$PLLA_{0.25}$	4.56	0.90	9.99	4.54	3.75	14.9
$PLLA_{0.5}$	4.98	0.90	13.47	13.3	4.84	500
$PLLA_1$	5.22	0.90	15.2	37.3	5.04	361

was found that the M_z/M_w was larger for cross-linked PHB and PLLA samples. However, the GDI values were significantly larger for cross-linked samples indicating that not only do they have a larger high molar mass component, but they also have a broader MWD at the low molar mass end (M_w/M_n). Therefore, it was important to examine HEI and GDI together, since both of these measures were sensitive to high molar mass fractions. The CPI was determined from G_c. CPI values have been reported to be in a good correlation with M_w/M_n for polypropylenes.[36] CPI, GDI, and HEI values of cross-linked PHB and PLLA, respectively, all increased with the extent of cross-linking. These data shows that DCP increased LCB.[10] Since the LCB favors chain entanglement over short chain branching (SCB) the melt elasticity is proportional to the degree of chain entanglement. Therefore, both G' and G'' were shown to increase significantly with DCP concentration (Figure 9) and LCB. The DRI is a measure of the shear sensitivity of viscosity, introduced by the Dow Chemical Company to characterize LCB for copolymers of ethylene and α-olefins made with INSITE technology metallocene catalysts,[37] and was not a meaningful measure for polymers whose viscosity was influenced by both MWD and LCB. DRI seems to fail for PHB_0 and $PLLA_0$ and their cross-linked polymers (Table IV).

All $PHB_{0–1}$ and $PLLA_{0–1}$ samples were also analyzed using the M_w/M_n viscosity function method on the steady shear viscosity data [as function of shear rate (γ)] at different temperatures. For these calculations the zero-shear viscosity (η_0) was estimated by the software program and not entered explicitly (Table IV). The two other parameters, polynomial order for the high γ fit and final slope magnitude, were set for all materials to be 2 and 0.75, respectively. The final slope magnitude was determined by decreasing its value from 1.0 until the weight distribution normalization values for all materials was as close as possible to 1.0. The η_0 of cross-linked PHB and PLLA were higher and increased with DCP concentration. D'Haene *et al.* had shown that DCP level < 0.3% resulted in cross-linked PHBV with a decreased η_0 and was similarly observed for low-density polyethylene (LDPE) as a result of high branching and a considerable decrease in the radius of gyration compared with the linear polymer[6]. Hence, it could be concluded the LCB formed in cross-linked PHB and PLLA polymer networks that would not lead to a decrease in the radius of gyration as compared with their linear polymers. The calculated values of M_w/M_n are given in Table IV. The M_w/M_n values were positively correlated with η_0 values. The computed M_w/M_n ratios of linear polymers were very close to SEC determined values. The values of M_w/M_n for both PHB and PLLA were shown to increase with DCP concentration or extent of cross-linking. In other words, the DCP induced cross-linking result in the broader MD and higher degree of LCB, which is consistent with the results of PD measures (HEI, GDI and CPI). The computed results show that PHB cross-linked with 1% DCP increased M_w/M_n two-fold, while for PLLA the M_w/M_n increased four-fold. The increase of the M_w/M_n with increasing peroxide concentration may be caused by an increasing amount of side chains and cross-links, resulting in a change in the weight average molar mass but not in the number-average molar mass.[13] For many polymers especially the ones with linear or SCB structures, the temperature dependence of rheological behavior can be described using a time shift factor, a_T, over a series of specific temperature, and a modulus shift factor, b_T, also known as time-temperature superposition (TTS). The time shift factor often follows the Arrhenius relation.[38]

$$a_T = \exp\ [(E_a/R)(1/T - T_0)] \quad (6)$$

where T is the absolute temperature, E_a is the activation energy of polymer melt, R is the gas constant and the subscript, "0,"

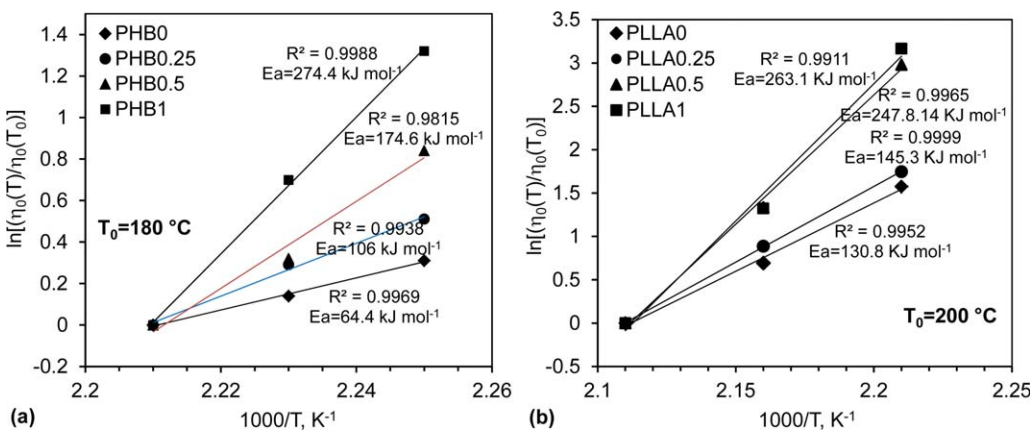

Figure 11. The effect of DCP concentration on the activation energy (E_a) of (a) PHB and (b) PLLA. [Color figure can be viewed in the online issue, which is available at wileyonlinelibrary.com.]

refers in all further discussion to an arbitrary reference temperature ($T_0 = 180$ and 200°C respectively for PHB and PLLA).

The RheoMWD analysis showed that LCBs formed upon DCP based cross-linking. TTS was shown to fail in the case of LCB materials with thermorheological complex behavior, which means that the effect of temperature cannot be described by a single time shift factor, and different shift factor is required at each time; hence the zero-shear viscosity was employed by Wood-Adams and Costeux for the LCB based polyethylene:

$$\hat{E}_0(T) = \eta_0(T_0) \exp\left[\left(\hat{E}_a/R\right)/(1/T - 1/T_0)\right] \quad (7)$$

where $\hat{E}_a$ is the apparent zero-shear rate activation energy, a weighted average of the material E_a.[38] The η_0 was estimated by RheoMWD at $T = 170$, 175, and 180°C for PHB, and $T = 180$, 190, and 200°C for PLLA. Using this approach the E_a based on η_0 were estimated by fitting the linearized form of eq. (7). The E_a was determined from the slope (slope $= \hat{E}_a/R$) versus $1/T$ of the fitted trend-line for LCB PHB and PLLA (Figure 11). Cross-linked PHB and PLLA polymers have higher E_a compared with their linear polymers. According to rheological studies there is a positive relationship between E_a and LCB for polyethylene.[38] Hence, it seems to be concluded that the higher LCB levels existed in the cross-linked polymer network, especially when >0.5% DCP were employed. Since LCB will enhance the shear thinning of a polymer melt (Figure 10), cross-linked $PHB_{0.25\text{-}1}$ and $PLLA_{0.25\text{-}1}$ showed more severe shear thinning than PHB_0 and $PLLA_0$. However, they also proposed that the combination of LCB with SCB also contribute to the thermorheological complex behavior. Therefore, the future work will be aimed at understanding the index of LCB and SCB, and how these will influence PHB and PLLA melt properties.

CONCLUSIONS

Free radical initiated cross-linking with DCP in the molten state proved to be an effective approach for modifying PHB and PLLA. The cross-linking reaction was verified to occur at tertiary carbon along the polymer chain. During cross-linking some chain scissioning also occurred, hence, to control the reaction time seems to be crucial to limit polymer degradation. Cross-linking resulted in a ductile material by lowering the polymer T_g, T_m, and χ_c (%), as well as reducing spherulite sizes. The cross-linked polymers were more thermally stable than linear polymers. Furthermore, the cross-linked PHB and PLLA materials had a broader MWD and LCB and thus showed improved melt strength. The cross-linked PHB and PLLA polymers could be potentially run at the higher line speeds and throughputs on industrial extrusion or foaming lines with minimum thermal degradation at lower cost because of lower heat input due to decrease of T_m and reduce the levels of plasticizers.

ACKNOWLEDGMENTS

The authors acknowledge (i) the support from a USDA-Forest Products Laboratory grant 08-JV-111111, (ii) Dr. Alexander Blumenfeld for his technical help with NMR, (iii) USDA-CSREES grants 2007-34158-17640 and 2005-35103-15243 for supporting the DSC/DMA and FTIR spectrometer, respectively, and (iv) Mr. Hugo Vuurens from Purac Netherlands for the PLLA sample.

REFERENCES

1. Rasal, R. M.; Janorkar, A. V.; Hirt, D. E. *Prog. Polym. Sci.* **2010**, *35*, 338.
2. Yu, L.; Dean, K.; Li, L. *Prog. Polym. Sci.* **2006**, *31*, 576.
3. Groot, W.; van Krieken, J.; Sliekersl, O.; de Voss, S. In Poly(Lactic Acid): Synthesis, Structures, Properties, Processing, and Applications, Auras, R., Lim, L.-T., Selke, S. E. M., Tsuji, H., Eds.; John Wiley & Sons, Inc.: Hoboken, New Jersey, **2010**; pp 1.
4. Lunt, J. *Polym. Degrad. Stab.* **1998**, *59*, 145.
5. Yamaguchi, M.; Arakawa, K. *Eur. Polym. J.* **2006**, *42*, 1479.
6. D'Haene, P.; Remsen, E. E.; Asrar, J. *Macromolecules* **1999**, *32*, 5229.
7. Roa, J. P.; Patrício, P. S. D. O.; Oréfice, R. L.; Lago, R. M. *J. Appl. Polym. Sci.* **2013**, *128*, 3019.
8. Wang, L.; Zhu, W.; Wang, X.; Chen, X.; Chen, G.-Q.; Xu, K. *J. Appl. Polym. Sci.* **2008**, *107*, 166.
9. Takamura, M.; Nakamura, T.; Kawaguchi, S.; Takahashi, T.; Koyama, K. *Polym. J. (Tokyo)*. **2010**, *42*, 600.
10. Ryan, C. M.; Hartmann, M. H.; Nangeroni, J. F. Polymers Laminations and Coatings Conference TAPPI Proceedings, **1997**, pp 139.
11. Dean, K. M.; Petinakis, E.; Meure, S.; Yu, L.; Chryss, A. *J. Polym. Environ.* **2012**, *20*, 741.
12. Nijenhuis, A. J.; Grijpma, D. W.; Pennings, A. J. *Polymer* **1996**, *37*, 2783.
13. Sijdergard, A.; Niemi, M.; Selin, J.-F.; Ngisman, J. H. *Ind. Eng. Chem. Res.* **1995**, *34*, 1203.
14. Yu, L.; Toikka, G.; Dean, K.; Bateman, S.; Yuan, Q.; Filippou, C.; Nguyen, T. *Polym. Int.* **2013**, *62*, 759.
15. Jandas, P. J.; Mohanty, S.; Nayak, S. K. *Ind. Eng. Chem. Res.* **2013**, *52*, 17714.
16. Fei, B.; Chen, C.; Chen, S.; Peng, S.; Zhuang, Y.; An, Y.; Dong, L. *Polym. Int.* **2004**, *53*, 937.
17. Takamura, M.; Nakamura, T.; Takahashi, T.; Koyama, K. *Polym. Degrad. Stab.* **2008**, *93*, 1909.
18. Khonakdar, H. A.; Morshedian, J.; Wagenknecht, U.; Jafari, S. H. *Polymer* **2003**, *44*, 4301.
19. De Koning, G. J. M.; Lemstra, P. J. *Polymer* **1993**, *34*, 4089.
20. Wei, L.; McDonald, A. G.; Freitag, C.; Morrell, J. J. *Polym. Degrad. Stab.* **2013**, *98*, 1348.
21. Solarski, S.; Ferreira, M.; Devaux, E. *Polymer* **2005**, *46*, 11187.
22. Wei, L.; Guho, N. M.; Coats, E. R.; McDonald, A. G. *J. Appl. Polym. Sci.* **2014**, *131*, 40333.
23. Hu, S.; McDonald, A. G.; Coats, E. R. *J. Appl. Polym. Sci.* **2013**, *129*, 1314.
24. Liu, B.; Png, R.-Q.; Zhao, L.-H.; Chua, L.-L.; Friend, R. H.; Ho, P. K. H. *Nat. Commun.* **2012**, *3*, 1321.
25. El-Hadi, A.; Schnabel, R.; Straube, E.; Müller, G.; Riemschneider, M. *Macromol. Mater. Eng.* **2002**, *287*, 363.
26. Goncalves, C. M. B.; Coutinho, J. A. P.; Marrucho, I. M. In Poly(lactic acid): Synthesis, Structures, Properties, Processing, and Applications, Auras, R., Lim, L.-T., Selke, S. E. M.,

Tsuji, H., Eds.; John Wiley & Sons, Inc.: Hoboken, New Jersey, **2010**; pp 97.

27. Kurniawan, L.; Qiao, G. G.; Zhang, X. *Biomacromolecules* **2007**, *8*, 2909.
28. Scandola, M.; Pizzoli, M.; Ceccorulli, G.; Cesaro, A.; Paoletti, S.; Navarini, L. *Int. J. Biol. Macromol.* **1988**, 373.
29. Gunaratne, L. M. W. K.; Shanks, R. A. *J. Polym. Sci., Part B: Polym. Phys.* **2006**, *44*, 70.
30. Hinüber, C.; Häussler, L.; Vogel, R.; Brünig, H.; Werner, C. *Macromol. Mater. Eng.* **2010**, *295*, 585.
31. Worzakowska, M. *J. Therm. Anal. Calorim.* **2010**, *101*, 685.
32. Nair, T. M.; Kumaran, M. G.; Unnikrishnan, G.; Pillai, V. B. *J. Therm. Anal. Calorim.* **2009**, *112*, 72.
33. Cocchini, F.; Nobile, M. R. *Rheol. Acta* **2003**, *42*, 232.
34. Ramkumar, D. H. S.; Bhatacharya, M. *Polym. Eng. Sci.* **1998**, *38*, 1426.
35. Shroff, R.; Mavridis, H. *J. Appl. Polym. Sci.* **1995**, *57*, 1605.
36. Zeichner, G. R.; Patel, P. D. The 2nd World Congress of Chemical Engineering, Montreal, Canada **1981**, p 333.
37. Pannier, G.; Chai, C. K. (Ineos Europe Ag) European Patent 2012/074792, June 20, **2013**.
38. Wood-Adams, P.; Costeux, S. P. *Macromolecules* **2001**, *34*, 6281.